Surface properties of solids using a semi-infinite approach and the tight-binding approximation

Hui Ou-Yang, Bruno Källebring, and R. A. Marcus Arthur Amos Noyes Laboratory of Chemical Physics,^{a)} California Institute of Technology, Pasadena, California 91125

(Received 1 September 1992; accepted 12 January 1993)

A semi-infinite approach (rather than a slab method or finite number of layers) is used to treat surface properties such as wave functions, energy levels, and Fermi surfaces of semi-infinite solids within the tight-binding (TB) approximation. Previous single-band results for the face-centered cubic lattice with a (111) surface and for the simple cubic lattice with a (001) surface are extended to semi-infinite layers, while the extension to calculations of other surfaces is straightforward. Treatment of more complicated systems is illustrated in the calculation of the graphite (0001) surface. Four interacting bands are considered in the determination of the wave functions, energies, and Fermi surface of the graphite (0001) surface. For the TB model used, the matrix elements in the secular determinants for the semi-infinite solid and for the infinite bulk solid obey the same expressions, and the wave functions are closely related. Accordingly, the results for the bulk system can then be directly applied to the semi-infinite one. The main purpose of the present paper is to provide wave functions and other properties used elsewhere to treat phenomena such as scanning tunneling microscopy and electron transfer rates at electrodes.

I. INTRODUCTION

A number of interrelated phenomena at surfaces include electron transfer processes at electrodes, scanning tunneling microscopy (STM) in the presence and absence of adsorbates, and electrochemical inverse photoemission. To aid in the understanding of these phenomena, electronic matrix elements are needed, such as those between the electrode and the acceptor or donor in electron transfers and between the metal or semiconductor surface and the tip in scanning tunneling microscopy. Surface properties such as the wave functions, energy levels, and Fermi surfaces have been used in our theoretical studies of the STM images of the graphite (0001) and Au(111) surfaces, and of large adsorbates on these surfaces. They are obtained for that purpose in the present paper.

To this end we employ the tight-binding (TB) method because of its simplicity. Earlier studies of electronic states of systems with surfaces using the TB method include that by Goodwin of a finite simple cubic crystal and of a finite linear chain,⁶ its extension by Baldock to face-centered and body-centered cubic lattices and to the hexagonal plane lattice,⁷ and by various authors to one-dimensional $ABAB\cdots$ solids and the face-centered cubic (111) surface with two interacting bands.⁸⁻¹⁴ In all of these calculations a finite number of layers in the lattice was used and the wave functions were normalized to a Kronecker delta, the normalization being to a "box" or using a Born-von Karman periodic boundary condition.

For a complicated system where there are several different types of atoms in the unit cell of the bulk and several orbitals in each atom, a slab calculation (limited number of layers) has been extensively employed to obtain the surface properties within the TB^{15(a)} and other^{15(b)} methods. The thickness of the slab was such as to ensure that it approximates a real surface, while being small enough to make the computation feasible. In the present paper a semi-infinite instead of a finite slab method is employed. Examples of more accurate methods used to treat surface properties include the Kohn–Sham density-functional theory. ^{16–18} Semi-infinite systems have been treated previously using various Green function and other techniques. ¹⁹

In the present paper, instead of a box type normalization⁸⁻¹⁴ for a finite system a Dirac delta function normalization²⁰ is used for several simple semi-infinite (surface) and infinite (bulk) three dimensional systems. (More complex systems can be treated systematically.20) The singleband face-centered-cubic (fcc) lattice with a (111) surface is treated in Sec. II B, for use in applications to electron transfer at Au(111) surface. [There is now a body of experimental electron transfer and STM studies at the Au(111) surface having monolayer adsorbates.²¹] Results for the (001) surface of the simple cubic (sc) lattice are briefly summarized for comparison. In Sec. II C the wave functions, energy levels, and Fermi energy surface for the graphite (0001) surface are determined, for use elsewhere in treating the STM images of adenine and thymine adsorbed on graphite surface.⁵ In the present paper we obtain a result for graphite, seen below but perhaps well known in the literature, on the identical nature of the secular equations for the surface and bulk systems, and the close relationship of the wave functions, for the present type of TB model. (The Hamiltonian matrices are identical only for an appropriate choice of Bloch orbital basis for the bulk solid. Otherwise these matrices are identical only after a unitary transformation.) This fact permits us to apply the extensive previous calculations on bulk studies to the

²⁾Contribution No. 8698.

present surface systems. A similar remark would apply to the other surfaces treated above.

II. THEORY

A. Remarks on infinite bulk system

We consider first an infinite three-dimensional periodic solid. In the case of one electronic orbital per unit cell, the electronic wave function for the solid in the TB approximation is

$$\Psi_{\mathbf{k}}(\mathbf{r}) = \sum_{l} e^{i\mathbf{k}\cdot\mathbf{r}_{l}}\phi(\mathbf{r}-\mathbf{r}_{l}),\tag{1}$$

using the Bloch theorem. In Eq. (1) \mathbf{r}_l is the lattice vector, $\mathbf{\Sigma}_{i=1}^3 l_i \mathbf{a}_i$, l denotes the triad $(l_1 l_2 l_3)$, \mathbf{k} is the wave vector, $\mathbf{\Sigma}_{i=1}^3 k_i \mathbf{b}_i$, \mathbf{a}_i , and \mathbf{b}_i denote the primitive and reciprocal lattice vectors, respectively, and satisfy $\mathbf{a}_i \cdot \mathbf{b}_j = 2\pi \delta_{ij}$, and $\phi(\mathbf{r} - \mathbf{r}_l)$ denotes an atomic wave function localized at \mathbf{r}_l . Once an origin for the atomic array has been arbitrarily selected, the position of any other atom in the system can be specified by the integers (l_1, l_2, l_3) . For normalization to a Dirac delta function²⁰ we have

$$\langle \Psi_{\mathbf{k}} | \Psi_{\mathbf{k}'} \rangle = \sum_{l} e^{i(\mathbf{k}' - \mathbf{k}) \cdot \mathbf{r}_{l}}$$

$$= \prod_{i=1}^{3} \sum_{l_{i}=-\infty}^{l_{i}=-\infty} e^{2\pi i l_{i}(k'_{i}-k_{i})} = \prod_{i=1}^{3} \delta(k'_{i}-k_{i}), \quad (2)$$

with $-\frac{1}{2} \le k_i \le \frac{1}{2}$. We have neglected overlap integrals of the ϕ 's, an approximation which is a convenient but not a necessary one.

B. Semi-infinite systems: Face-centered cubic (111) and simple cubic (001) surfaces

1. General

For a semi-infinite solid, the periodicity in the direction along the unit cell leading from the surface to the interior of the solid is destroyed by the presence of the surface, and the Bloch theorem is no longer applicable for that direction. However, utilizing the results and method of the one-dimensional solution, the wave function for all three directions is obtained for this semi-infinite case: Throughout this paper the particular examples we consider are those in which every plane parallel to the surface has the same two-dimensional space group.

The wave functions for a semi-infinite solid can be written in the TB approximation as the linear combinations of the Bloch functions for the individual layers parallel to the surface,

$$\Psi_k(\mathbf{r}) = \sum_{l_1 l_2 l_3} c_{l_3} e^{ik \| \mathbf{r} \cdot \mathbf{r}_l \phi(\mathbf{r} - \mathbf{r}_l)}, \tag{3}$$

where c_{l_3} denotes the coefficient corresponding to the l_3 th layer parallel to the surface, $\sum_{l_1 l_2} e^{i\mathbf{k}_{\parallel} \cdot \mathbf{r}_{l}} \phi(\mathbf{r} - \mathbf{r}_{l})$ serves as the Bloch wave function for the l_3 th layer, \mathbf{k}_{\parallel} denotes $k_1\mathbf{b}_1 + k_2\mathbf{b}_2$, and then $\mathbf{k}_{\parallel} \cdot \mathbf{r}_{l} = 2\pi(k_1l_1 + k_2l_2)$.

Introducing Eq. (3) for Ψ into the Schrödinger equation, $H\Psi = E\Psi$, multiplying by $e^{-ik_{\parallel} \cdot \mathbf{r} \cdot \mathbf{r}} \phi^*(\mathbf{r} - \mathbf{r}_{l'})$, inte-

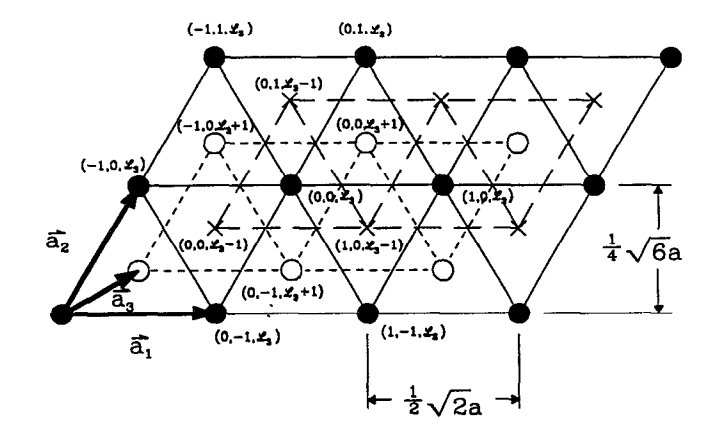


FIG. 1. The geometry of the fcc (111) surface. Solid circles are located on l_3 th layer, open circles on (l_3+1) th layer, and crosses on (l_3-1) th layer. All (l_1,l_2) coordinates are relative to a particular atom.

grating over r, using the nearest-neighbor approximation, and neglecting overlap integrals, a system of difference equations is obtained,

$$\left[(H_{ll} - E) + \sum_{l_1 l_2} ' e^{i\mathbf{k}_{\parallel} \cdot (\mathbf{r}_{l} - \mathbf{r}_{l'})} H_{ll'} \right] c_{l'_3}
+ \sum_{l_1 l_2} '' e^{i\mathbf{k}_{\parallel} \cdot (\mathbf{r}_{l} - \mathbf{r}_{l'})} H_{ll'} c_{l'_3 + 1} + \sum_{l_1 l_2} ''' e^{i\mathbf{k}_{\parallel} \cdot (\mathbf{r}_{l} - \mathbf{r}_{l'})} H_{ll'} c_{l'_3 - 1}
= 0, \quad l'_3 = 1, 2, 3, ..., \tag{4}$$

where $H_{ls} = \langle \phi(\mathbf{r}_l) | H | \phi(\mathbf{r}_s) \rangle$, s = l, l'. Dirac notation has been introduced and $|\phi(\mathbf{r}_s)\rangle$ denotes a ϕ ket localized at \mathbf{r}_s . The primed, double primed, and triple primed sums are over nearest neighbors $l_1 l_2$ of an atom (l'_1, l'_2, l'_3) in the same layer $(l_3 = l'_3)$, or in the layer below $(l_3 = l'_3 + 1)$, or in the layer above $(l_3 = l'_3 - 1)$, respectively. For the surface layer $(l_3 = 1)$, serving as a boundary condition, c_0 is defined to be zero in Eq. (4).

The results obtained below for the cubic systems are each for a single-band solid consisting of s orbitals. A surface calculation for a multiband solid with more general orbitals is somewhat more involved. There, each band i has a coupling parameter F_i , which may be complex valued. A systematic treatment for multiple bands with complex F_i can be made as in Ref. 20(a).

2. Face-centered cubic (111) surface

We consider an fcc(111) surface where ϕ denotes an s state of an individual atom, as in Au(111), for example. H_{ll} is denoted by α and $H_{ll'}$ by β whenever l and l' are nearest neighbors. (The parameters α and β are assumed to be the same for the surface layer and the interior layers, thereby neglecting Tamm surface states.⁶) There are six nearest atoms in the same layer, three in the layers below and, except for the surface layer, three in the layers above, as in Fig. 1. The primed, double primed, and triple primed sums in Eq. (4) equal $2[\cos 2\pi k_1 + \cos 2\pi k_2 + \cos 2\pi (k_1 - k_2)]$ ($l'_3 = l_3$), $e^{2\pi i k_2} + e^{2\pi i k_1} + 1 \equiv F/\beta$ ($l'_3 = l_3 + 1$), and F^*/β ($l'_3 = l_3 - 1$), respectively, where we have introduced

an abbreviated notation F/β for the indicated sum and where the asterisk denotes complex conjugate.

Equation (4) thus becomes

$$(E_s - E)c_{l_3} + Fc_{l_2+1} + F^*c_{l_3-1} = 0, (5)$$

where E_s equals $\alpha + 2\beta[\cos 2\pi k_1 + \cos 2\pi k_2 + \cos 2\pi (k_1 - k_2)]$, with $c_0 = 0$ when Eq. (5) is used for the surface layer $(l_3 = 1)$. The well-known solutions of Eq. (5) are²³

$$E=E_s+2|F|\cos 2\pi k_3 l_3$$
, $c_{l_3}=(|F|/F)\sin 2\pi k_3 l_3$, (6)

where k_3 is any real number in the interval $(0,\frac{1}{2})$. The wave functions $\Psi_{\mathbf{k}}(\mathbf{r})$ for a solid having an fcc(111) surface are thus given by

$$\Psi_{k}(\mathbf{r}) = \sqrt{2} \sum_{l_{3}=1}^{\infty} (|F|/F)^{l_{3}} \sin 2\pi k_{3} l_{3}$$

$$\times \sum_{l_{1}, l_{2}=-\infty}^{\infty} e^{2\pi i (k_{1} l_{1} + k_{2} l_{2})} \phi(\mathbf{r} - \mathbf{r}_{l}), \tag{7}$$

where $\Psi_{\mathbf{k}}(\mathbf{r})$ is normalized as in Eq. (2).

These results will be used elsewhere in the treatment of electron transfer rates across adsorbates on Au(111) surfaces.

3. Simple cubic (001) surface

For an sc(001) solid there are four nearest l atoms for l' atom in the same layer, there is one atom below and, except for the surface layer, one atom above. The primed, double primed, and triple primed sums in Eq. (4) are now equal to $2(\cos 2\pi k_1 + \cos 2\pi k_2)$, $\sum_{l_1,l_2} e^{2\pi i [k_1(l_1-l_1')+k_2(l_2-l_2')]} = 1$ (since $l_1 - l_1' = l_2 - l_2' = 0$), and 1 for the same reason, respectively. The solutions to Eq. (4) again yield Eqs. (6) and (7), but with F and F^* both replaced by β , and with E_s now being $\alpha + 2\beta(\cos 2\pi k_1 + \cos 2\pi k_2)$. (The parameters α and β were again assumed to be the same for the surface layer and the interior layers.) k_3 is again any real number in the interval $(0,\frac{1}{2})$.

C. Graphite (0001) surface

1. Bulk graphite

We first review briefly the TB treatment of bulk graphite, and then treat the graphite (0001) surface. The properties of bulk graphite have been determined both experimentally and theoretically.²⁴

The Bernal structure 25 is typically used in band structure calculations of graphite. The crystal structure of graphite is shown in Fig. 2. The unit cell contains four carbon atoms, α , β , α' , and β' , with two atoms each in adjacent planes. The in-plane distance between nearest carbon atoms is 1.42 Å and the carbon planes are separated by 3.35 Å. The unit cell and the Brillouin zone are depicted in Figs. 3 and 4, respectively.

Band structure calculations of bulk graphite have been extensively performed.^{24,26-37} Within the TB domain, the calculation most widely used to interpret the physical properties of graphite has been given by Slonczewski and

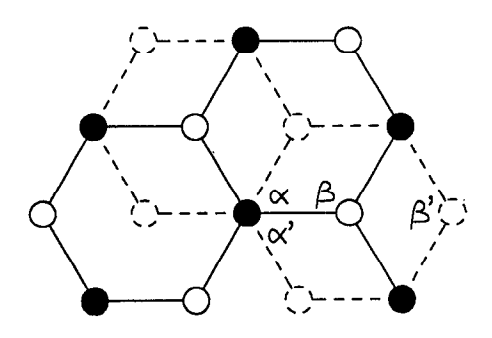


FIG. 2. Schematic drawing of the atomic structure of graphite. The solid lines show one layer and the dashed lines show an adjacent layer. The α -type atoms in this second layer are α' and are, as indicated, above or below each α atom.

Weiss (SW). 30 It is well established both experimentally 24 and theoretically $^{24,26-30}$ that the electronic properties of graphite are effectively determined by the four interacting π bands consisting of only p_z orbitals. Two of the π bands are fully occupied, and the other two are empty. Near the edges in the Brillouin zone, the four π bands lie close to each other and to the Fermi level. In the Slonczewski–Weiss (SW) model only the π bands in the neighborhood of the zone edges, where the Fermi energy E_f occurs, are calculated, instead of making a complete calculation of the band structure.

The Bloch wave functions arising from the p_z orbitals of the four carbon atoms, α , β , α' , and β' , are given for the bulk solid by

$$\Phi_{\mathbf{k}}^{j}(\mathbf{r}) = \sum_{l} e^{i\mathbf{k}\cdot\mathbf{r}_{l}^{j}} p_{z}(\mathbf{r} - \mathbf{r}_{l}^{j}) \quad (j = \alpha, \beta, \alpha', \beta'). \tag{8}$$

The wave functions $\Psi_k(\mathbf{r})$ are then approximated by linear combinations of these Bloch wave functions

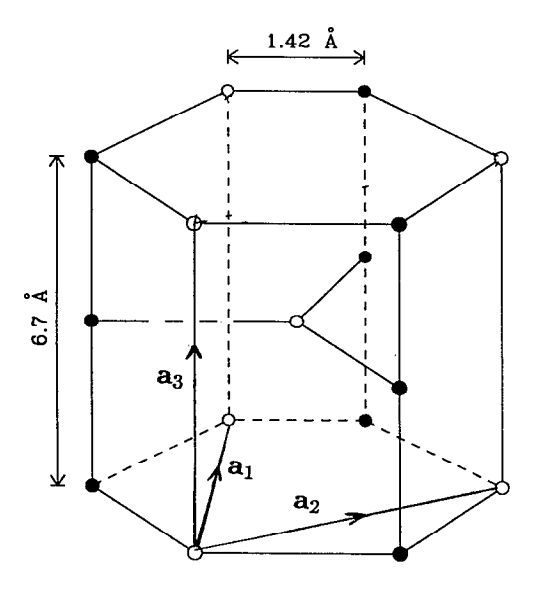


FIG. 3. Unit cell of graphite. In the top and lowest layer full circles represent α atoms and empty circles β atoms. In the middle layer they represent α' and β' atoms.

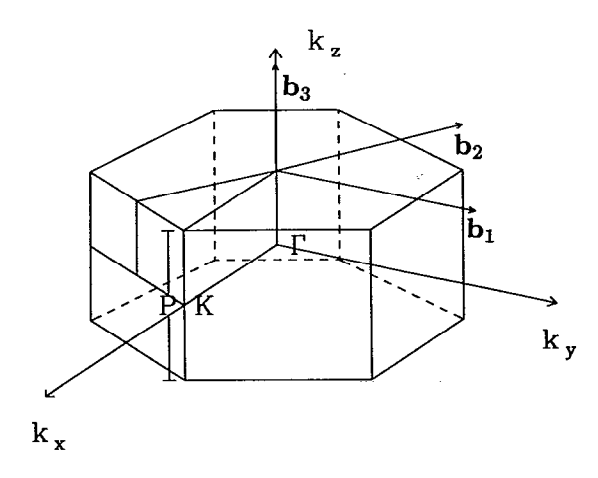


FIG. 4. The Brillouin zone of graphite.

$$\Psi_{\mathbf{k}}(\mathbf{r}) = \sum_{j} c_{j}(\mathbf{k}) \Phi_{\mathbf{k}}^{j}(\mathbf{r}), \tag{9}$$

where the sum is over $j = \alpha$, β , α' , and β' .

The 4×4 Hamiltonian matrix is then given by

$$H = \begin{pmatrix} H_{\alpha\alpha} & H_{\alpha\beta} & H_{\alpha\alpha'} & H_{\alpha\beta'} \\ H_{\beta\alpha} & H_{\beta\beta} & H_{\beta\alpha'} & H_{\beta\beta'} \\ H_{\alpha'\alpha} & H_{\alpha'\beta} & H_{\alpha'\alpha'} & H_{\alpha'\beta'} \\ H_{\beta'\alpha} & H_{\beta'\beta} & H_{\beta'\alpha'} & H_{\beta'\beta'} \end{pmatrix}, \tag{10}$$

where $H_{\alpha'\alpha'} = H_{\alpha\alpha}$, $H_{\beta'\beta'} = H_{\beta\beta}$, and this H_{ij} matrix is Hermitian. The one-electron Hamiltonian of the graphite lattice can be written as $H = H_0 + H'$, where H_0 denotes the Hamiltonian for an isolated carbon atom, H' is V - U, U is the potential field for an isolated atom, and V is the periodic potential of the lattice.

The matrix elements in Eq. (10) are given by

$$H_{ii} = E_0 - \Delta_i + 2\gamma_{ii} \cos 2\pi k_3 \quad (i = \alpha, \beta, \alpha', \beta'), \tag{11}$$

$$H_{\alpha\beta} = H_{\beta'\alpha'} = \gamma_{\alpha\beta}F_2(\mathbf{k}_{\parallel}), \quad H_{\alpha\alpha'} = 2\gamma_{\alpha\alpha'}\cos\pi k_3, \quad (12)$$

$$H_{\alpha\beta'}=H_{\beta\alpha'}=2\gamma_{\alpha\beta'}F_2^*(\mathbf{k}_{\parallel})\cos\pi k_3$$

$$H_{BB'} = 2\gamma_{BB'}F_2(\mathbf{k}_{\parallel})\cos\pi k_3. \tag{13}$$

In Eqs. (11)–(13) E_0 is the energy of the $2p_z$ electron for an isolated carbon atom, $\gamma_{ij} = \langle p_z(\mathbf{r}_i) | H' | p_z(\mathbf{r}_j) \rangle$, $\gamma_{ii} = \langle p_z(\mathbf{r}_i) | H' | p_z(\mathbf{r}_i + \mathbf{a}_3) \rangle$, $\Delta_i = -\langle p_z(\mathbf{r}_i) | H' | p_z(\mathbf{r}_i) \rangle$, where $i, j = \alpha, \beta, \alpha', \beta'$, and $\gamma_{\alpha\beta}, \gamma_{\alpha\alpha'}, \gamma_{\beta\beta}, \gamma_{\beta\beta'}, \gamma_{\alpha\beta'}$, and $\gamma_{\alpha\alpha}$ are known as γ_i (i = 0 to 5) in the literature, respectively. $F_2(\mathbf{k}_{\parallel})$ denotes $\Sigma_{i=1}^3 \exp(i\mathbf{k}_{\parallel} \cdot \mathbf{A}_0 \mathbf{B}_i)$, where $\mathbf{k}_{\parallel} = k_1 \mathbf{b}_1 + k_2 \mathbf{b}_2$, and where the orientations of \mathbf{b}_1 and \mathbf{b}_2 , and three vectors, $\mathbf{A}_0 \mathbf{B}_i$, are given in Figs. 4 and 5, respectively. The value of F_2 is given in Ref. 38. For a point in the vicinity of the zone edge, $F_2(\mathbf{k}_{\parallel})$ in the SW model can be evaluated by an accurate first-order expansion about the zone edge, $f_2(\mathbf{k}_{\parallel})$ although we do not use this approximation. In the subsequent expressions the \mathbf{k}_{\parallel} is omitted from the $F_2(\mathbf{k}_{\parallel})$ for notational brevity.

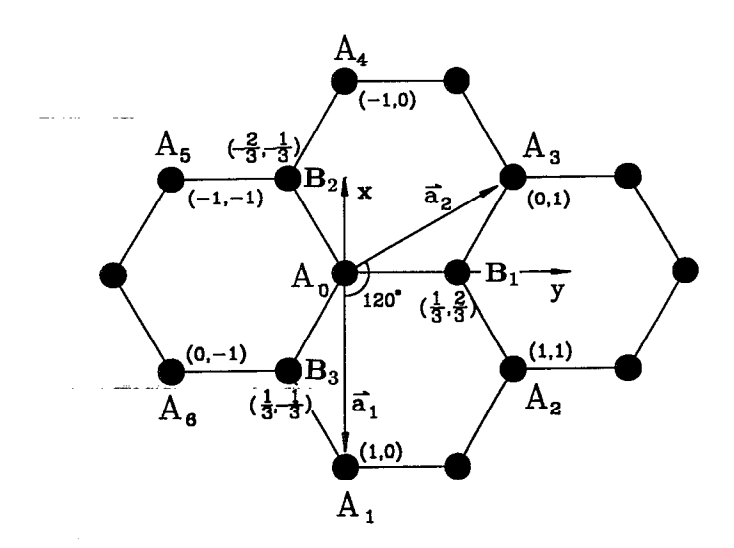


FIG. 5. Plane graphite. A and B represent α and β atoms, respectively. All (I_1,I_2) coordinates are relative to the A_0 atom.

After a unitary transformation on the Hamiltonian matrix in Eq. (10), 24,30 the SW Hamiltonian $H_{\rm sw}{=}S^{-1}HS$ is obtained, with

$$S = \begin{bmatrix} \frac{1}{\sqrt{2}} & \frac{1}{\sqrt{2}} & 0 & 0\\ 0 & 0 & 1 & 0\\ \frac{1}{\sqrt{2}} & \frac{-1}{\sqrt{2}} & 0 & 0\\ 0 & 0 & 0 & 1 \end{bmatrix}, \tag{14}$$

where two of the matrix elements in $H_{\rm SW}$ vanish, and the expressions for the remaining ones are given, e.g., in Refs. 24 and 30. The band structure, wave functions, Fermi surface, and other properties of the bulk graphite can be determined using $H_{\rm SW}$.

2. Graphite with the (0001) surface

The difference between a surface and its bulk lies in the periodicity in the direction away from the surface. As in the bulk, there are four types of carbon atoms for the case of the (0001) surface, corresponding to α , β , α' , and β' . In the TB treatment, the wave function for this system can be written as a linear combination of two-dimensional Bloch functions for α , β , α' , and β' , respectively,

$$\Psi = \sum_{s=\alpha\beta} \sum_{l_3=1}^{\infty} \sum_{l_1 l_2} c_{l_3}^s e^{i\mathbf{k} \| \cdot r_l^s} p_z(\mathbf{r} - \mathbf{r}_l^s)$$

$$+ \sum_{t=\alpha',\beta'} \sum_{l_2=2}^{\infty} \sum_{l_1 l_2} c_{l_3}^t e^{i\mathbf{k} \| \cdot r_l^t} p_z(\mathbf{r} - \mathbf{r}_l^t), \qquad (15)$$

where the sum over l_3 is over odd integers in the first term and over even integers in the second, $\mathbf{r}_l^{\mu} = l_1^{\mu} \mathbf{a}_1 + l_2^{\mu} \mathbf{a}_2 + l_3^{\mu} \mathbf{a}_3$, $l_3^{\mu} = 1$, 3, 5,... for $\mu = s$ and $l_3^{\mu} = 2$, 4, 6,... for $\mu = t$. Layers 1, 3, 5,... contain α and β atoms, and 2, 4, 6,... contain α' and β' atoms. \mathbf{a}_1 , \mathbf{a}_2 , \mathbf{a}_3 are depicted in Fig. 3, and several values

of l_1^{α} , l_2^{α} , l_1^{β} , and l_2^{β} are given in Fig. 5. For notational brevity, l_i has been used to denote l_i^{μ} , where i=1, 2, 3.

Introducing Ψ into the Schrödinger equation, $H\Psi=E\Psi$, where H is the Hamiltonian for the present system, multiplying on the left side with $e^{-i\mathbf{k}_{\parallel}\cdot\mathbf{r}_{p}^{i}}p_{z}^{*}(\mathbf{r}-\mathbf{r}_{p}^{i})$, where $i=\alpha$ or β , integrating, and using the nearest neighbor approximation, we obtain

$$\sum_{s=\alpha\beta} \sum_{l_1 l_2} c_{l_3}^s e^{i\mathbf{k}_{\parallel} \cdot (\mathbf{r}_l^s - \mathbf{r}_{l'}^i)} \langle p_z(\mathbf{r}_{l'}^i) | H | p_z(\mathbf{r}_l^s) \rangle
+ \sum_{t=\alpha'\beta'} \sum_{l_1 l_2 l_3''} c_{l_3''}^t e^{i\mathbf{k}_{\parallel} \cdot (\mathbf{r}_{l_1 l_2 l_3''}^t - \mathbf{r}_{l_1' l_2' l_3''}^i)} \langle p_z(\mathbf{r}_{l'}^i) | H | p_z(\mathbf{r}_{l_1 l_2 l_3''}^t) \rangle
= E c_{l'}^i, \quad (i=\alpha,\beta)$$
(16)

upon introducing Dirac notation. The sum over l_3^v contains two terms, $l_3^v = l_3^v - 1$ and $l_3^v + 1$. For notational brevity, we replace the matrix elements in Eq. (16) with the Hamiltonian parameters defined earlier. With some manipulation⁴⁰ Eq. (16) becomes

$$\sum_{s=\alpha\beta} (h_{is} - E\delta_{is}) c_{i'_3}^s + \sum_{t=\alpha'\beta'} h_{it} (c_{i'_3+1}^t + c_{i'_3-1}^t) = 0,$$

$$i = \alpha, \beta, \quad l'_3 = 1, 3, 5, \dots$$
(17a)

Similarly, the difference equations for the α' and β' atoms are found to be

$$\sum_{s=\alpha'\beta'} (h_{is} - E\delta_{is}) c_{l_3'}^s + \sum_{t=\alpha\beta} h_{it} (c_{l_3'+1}^t + c_{l_3'-1}^t) = 0,$$

$$i = \alpha', \beta', \quad l_3' = 2, 4, 6, \dots,$$
(17b)

where we interchanged the dummy variables s and t, to emphasize the similarity of Eqs. (17a) and (17b). In Eq. (17a) c_0^t =0, and in Eqs. (17a) and (17b) $h_{\mu\mu}$ and $h_{\mu\nu}$ equal to $H_{\mu\mu}$ and $H_{\mu\nu}$ in Eqs. (11)–(13) with $\gamma_{\mu\mu}$ in $H_{\mu\mu}$ and $2\cos\pi k_3$ in $H_{\mu\nu}$ replaced by zero and 1, respectively, and where μ , ν = α , β , α' , β' .

To solve Eqs. (17a) and (17b), we first consider a special case in which the atoms α and α' do not interact with β and β' . The difference equations for the model systems (α,α') and (β,β') are obtained from Eqs. (17a) and (17b) by setting the relevant parameters for the interaction of the (α,α') and (β,β') systems, $\gamma_{\alpha\beta}$ and $\gamma_{\alpha\beta'}$, equal to zero. The equations for the (α,α') system then become

$$(h_{\alpha\alpha} - E)c_{l'_3}^{0\alpha} + h_{\alpha\alpha'}(c_{l'_3+1}^{0\alpha'} + c_{l'_3-1}^{0\alpha'}) = 0, \quad l'_3 = 1,3,5,... \quad (18a)$$

and

$$(h_{\alpha'\alpha'}-E)c_{l'_3}^{0\alpha'}+h_{\alpha'\alpha}(c_{l'_3+1}^{0\alpha}+c_{l'_3-1}^{0\alpha})=0, \quad l'_3=2,4,6,...,$$
(18b)

where superscript 0 denotes the model system (α, α') . In Eq. (18a) $c_0^{0\alpha'} = 0$.

Equations (18a) and (18b) are the difference equations for the model system

$$\alpha - \alpha' - \alpha - \alpha' - \alpha - \alpha' \cdots$$

a semi-infinite chain consisting of two different types of atoms α and α' , where $h_{\alpha\alpha}$ and $h_{\alpha\alpha'}$ are the Coulomb and resonance (hopping) integrals, respectively. The solutions of Eqs. (18a) and (18b), obtained in the Appendix, are

$$c_{l_3}^{0\gamma} = A_{\gamma} \sin \pi k_3 l_3 \quad (\gamma = \alpha, \alpha'), \tag{19a}$$

where $l_3=1,3,5,...$ for $\gamma=\alpha$ and $l_3=2,4,6,...$ for $\gamma=\alpha'$, $0 < k_3 < \frac{1}{2}$, and A_{γ} is given in Eqs. (A7) and (A8). Similarly, $c_{l_3}^{0\beta}$ and $c_{l_3}^{0\beta'}$ are given by

$$c_{l_3}^{0\gamma} = A_{\gamma} \sin \pi k_3 l_3, \quad (\gamma = \beta, \beta'), \tag{19b}$$

where $l_3 = 1,3,5,...$ for $\gamma = \beta$ and $l_3 = 2,4,6,...$ for $\gamma = \beta'$.

Considering next the interaction of the (α,α') and (β,β') systems, the solutions of the difference equations (17a) and (17b) are taken to be the linear combination of the solutions of the corresponding noninteracting systems, namely a linear combination of the following four coefficients:

$$c_{l_2}^s = 2Q_s \sin \pi k_3^s l_3, \qquad (20)$$

where $l_3=1,3,5,...$ for $s=\alpha$, β , $l_3=2,4,6,...$ for $s=\alpha'$, β' , $0 < k_3^s < 1/2$, and where we then seek a solution for the Q's. Introduction of Eq. (20) for $c_{l_3}^s$ into Eqs. (17a) and (17b) leads to four linear equations, upon reconstituting the H_{ij} from the h_{ij}

$$\sum_{j} (H_{ij} - E\delta_{ij}) Q_{j} = 0, \quad i = \alpha, \beta, \alpha', \beta', \tag{21}$$

where j is summed over the four atoms, α , β , α' , β' , and where the relation $c_{l_3+1}^s + c_{l_3-1}^s = 2Q_s[\sin \pi k_3^s(l_3+1) + \sin \pi k_3^s(l_3-1)] = 4Q_s \sin \pi k_3^s l_3 \cos \pi k_3^s$ has been used $(s=\alpha,\beta,\alpha',\beta')$.

The expressions for the matrix elements that appear in Eq. (21) are identical to those in Eqs. (11)–(13) for the bulk graphite, even though the original Bloch orbital basis set differed in the two cases, one being the normal Bloch wave functions, and the other being, in the case of a perfect semi-infinite graphite (0001) surface, the wave functions given in Eqs. (15) and (20). Thus using the same values of the parameters, the procedure of calculating the surface properties are the same as that for calculating the bulk properties in the SW model.

The simultaneous solutions of Eq. (21) require that the 4×4 determinant of the coefficients vanish, namely,

$$\begin{vmatrix} H_{\alpha\alpha} - E & H_{\alpha\beta} & H_{\alpha\alpha'} & H_{\alpha\beta'} \\ H_{\beta\alpha} & H_{\beta\beta} - E & H_{\beta\alpha'} & H_{\beta\beta'} \\ H_{\alpha'\alpha} & H_{\alpha'\beta} & H_{\alpha'\alpha'} - E & H_{\alpha'\beta'} \\ H_{\beta'\alpha} & H_{\beta'\beta} & H_{\beta'\alpha'} & H_{\beta'\beta'} - E \end{vmatrix} = 0, \quad (22)$$

in which the overlap integrals were neglected and from which the energy levels are calculated. The H_{ij} matrix, it will be recalled, is Hermitian. Again, after a unitary transformation of the Hamiltonian matrix using Eq. (14), ^{24,30} the solution of Eq. (22) yields the values of E and, in the

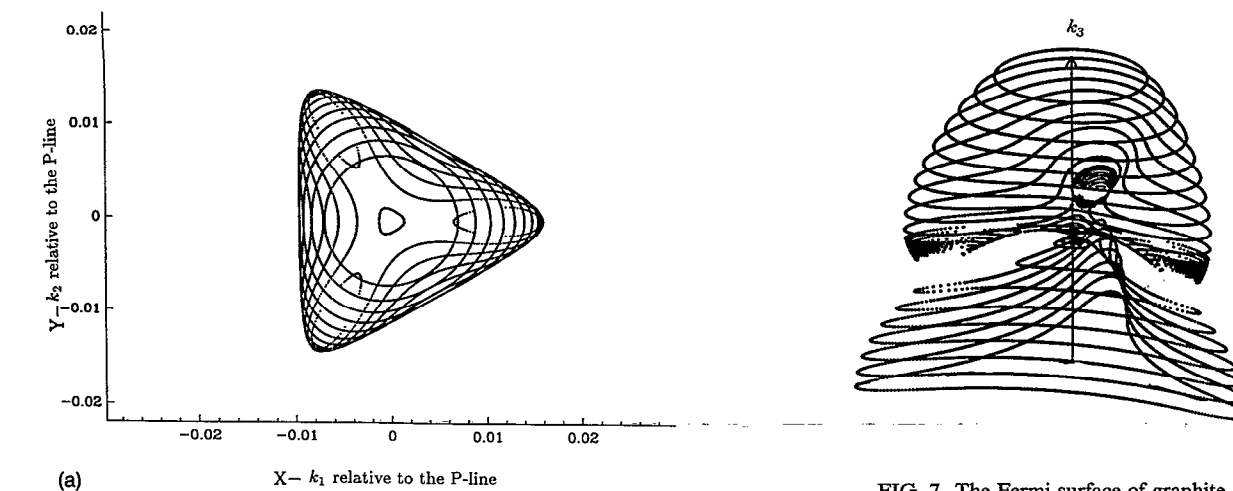


FIG. 7. The Fermi surface of graphite.

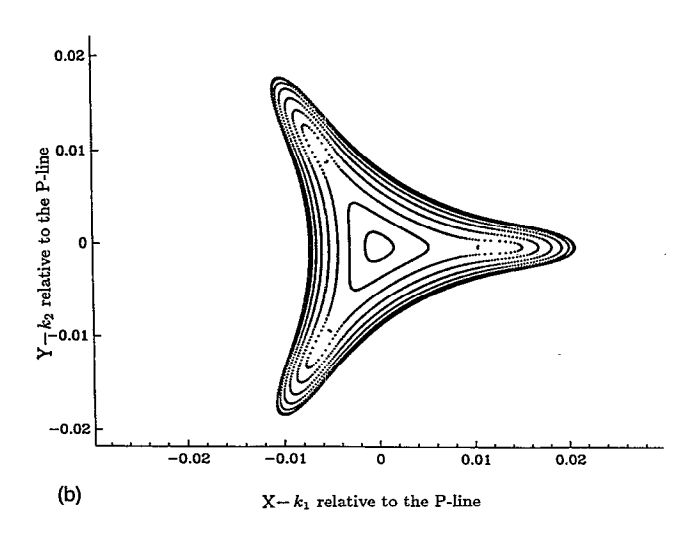


FIG. 6. Cross sections of the Fermi surface (a) for electrons and (b) for holes. Each contour corresponds to a particular k_3 value.

usual way therefore, of the Q^{α} , Q^{β} , $Q^{\alpha'}$, and $Q^{\beta'}$ in Eq. (21). We have $\sum_{i}Q_{i}^{2}=1$, resulting from the Dirac normalization, where sum is over $j = \alpha, \beta, \alpha', \beta'$.

For the purposes of comparing with the scanning tunneling microscopy (STM) experimental studies of graphite, we have calculated energies, wave functions, and Fermi surface, all of which are used in the interpretation of the STM images. The cross sections of the Fermi surface, and the Fermi surface itself are shown in Figs. 6 and 7, respectively. The SW parameters and the corresponding surface parameters employed in the present calculations are taken to be the same and can be found in references such as Refs. 24 and 30. In a subsequent article, the Fermi surfaces of the bulk graphite and gold are also determined,⁴¹ using the extended Hückel method.42

In conclusion, in the course of solving the semi-infinite difference equations for graphite with a (0001) surface in which four bands are considered, the difference equations are reduced to four linear equations, yielding a 4×4 determinant and the corresponding secular equations for the energy levels for the semi-infinite surface, and then yielding the wave functions. The calculational procedure is other-

wise the same as that for the bulk. As noted earlier, application of the present work to STM images will be described in a further publication.⁴

ACKNOWLEDGMENTS

It is a pleasure to acknowledge the support of this research by the Office of Naval Research, by the National Science Foundation, and in the form of a post-doctoral fellowship to B.K., by the Natural Science Research Council of Sweden.

APPENDIX: SOLUTIONS OF EQS. (18a) AND (18b)

Following Ref. 11, we rewrite Eqs. (18a) and (18b) as

$$(X-Z_1)c_{l_3}^{0\alpha} = c_{l_3-1}^{0\alpha'} + c_{l_3+1}^{0\alpha'}, \quad l_3 = 3,5,7,...,$$
 (A1)

$$(X+Z_1)c_{l_2}^{0\alpha'}=c_{l_2-1}^{0\alpha}+c_{l_2+1}^{0\alpha}, \quad l_3=2,4,6,...,$$
 (A2)

$$(X-Z_1)c_2^{0\alpha'} = \frac{1}{(X+Z_1)} (c_3^{0\alpha} + c_1^{0\alpha}).$$
 (A3)

In Eqs. (A1)-(A3) X and Z_1 are defined as $X=(E-\bar{\alpha})/$ $\gamma_{\alpha\alpha'}$, $Z_1 = (\alpha_{\alpha} - \alpha_{\alpha'})/2\gamma_{\alpha\alpha'}$, where $\bar{\alpha} = (\alpha_{\alpha} + \alpha_{\alpha'})/2$, α_i $=E_0-\Delta_i$ $(i=\alpha,\alpha').$

Equations (A1)-(A3) are the difference equations for the semi-infinite one-dimensional system depicted four lines after Eq. (18b). Similar systems have been treated in Ref. 11. Following Ref. 11, the solutions of Eqs. (A1)-(A3) are found by setting

$$c_{l_3}^{0\alpha} = U^{l_3}$$
, $l_3 = 1,3,5,...$; $c_{l_3}^{0\alpha'} = V^{l_3}$, $l_3 = 2,4,6,...$ (A4)

Introducing Eq. (A4) for $c_{l_3}^{0\alpha}$ and $c_{l_3}^{0\alpha'}$ into Eqs. (A1) and (A2) and eliminating V leads to

$$U^4 - \gamma U^2 + 1 = 0, (A5)$$

where $\gamma = X^2 - Z_1^2 - 2$. Choosing $\gamma = 2 \cos 2\pi k_3$ means that the general solution can be written as¹¹

$$c_{l_3}^{0\alpha} = p \cos \pi k_3 l_3 + q \sin \pi k_3 l_3, \quad l_3 = 1,3,5,....$$
 (A6)

It can be shown that introducing Eq. (A6) into Eq. (A3) gives p=0. We therefore obtain

$$c_{l_3}^{0\alpha} = q \sin \pi k_3 l_3, \quad l_3 = 1,3,5,...$$
 (A7)

and

$$c_{l_3}^{0\alpha'} = \frac{1}{(X+Z_1)} \left(c_{l_3+1}^{0\alpha} + c_{l_3-1}^{0\alpha} \right)$$

$$= q \frac{2_{\alpha\alpha'}}{(E-\alpha_{\alpha'})} \cos \pi k_3 \sin \pi k_3 l_3, \quad l_3 = 2,4,6...,$$
(A8)

where q is the normalization factor. Equations (A7) and (A8) are the same as Eqs. (19a) and (19b) in the text if qand $2q\gamma_{\alpha\alpha'}\cos\pi k_3/(E-\alpha_{\alpha'})$ are replaced with A_{α} and $A_{\alpha'}$, respectively. As in Ref. 20(a) the wave function can be normalized to a Dirac delta function.

- ¹For reviews, see R. A. Marcus, Ann. Rev. Phys. Chem. 15, 155 (1964); R. A. Marcus and N. Sutin, Biochim. Biophys. Acta. 811, 265 (1985); Reactions of Molecules at Electrodes, edited by N. S. Hush (Wiley, New York, 1971); N. Sutin, Prog. Inor. Chem. 30, 441 (1983); M. D. Newton and N. Sutin, Ann. Rev. Phys. Chem. 35, 437 (1984); K. V. Mikkelsen and M. A. Ratner, Chem. Rev. 87, 113 (1987); M. D. Newton, ibid. 91, 767 (1991); J. R. Bolton, N. Mataga, and G. McLendon (eds.), Adv. Chem. Ser. 228, assorted articles (1991).
- ²For reviews, see G. Binnig and H. Rohrer, Rev. Mod. Phys. 59, 615 (1987); P. K. Hansma and J. Tersoff, J. Appl. Phys. 61, R1 (1987); N. D. Lang, Comments Condens. Matter Phys. 14, 253 (1989); in Scanning Tunneling Microscopy and Related Methods, edited by R. J. Behm, N. Garcia, and H. Rohrer (Kluwer Academic, Dordrecht, 1990); M. Tsukada, K. Kobayashi, N. Isshiki, and H. Kageshima, Surf. Sci. Rep. 13, 265 (1991).
- ³ For reviews, see V. Dose, Surf. Sci. Rep. 5, 337 (1985); F. J. Himpsel, Comments Condens. Matter Phys. 12, 199 (1986); N. V. Smith, Rep. Prog. Phys. 51, 1227 (1988); F. J. Himpsel, Surf. Sci. Rep. 12, 1 (1990).
- ⁴H. Ou-Yang, B. Källebring, and R. A. Marcus, J. Chem. Phys. (to be
- ⁵H. Ou-Yang, B. Källebring, and R. A. Marcus (unpublished).
- ⁶E. T. Goodwin, Proc. Cambridge Philos. Soc. 35, 205 (1939).
- ⁷G. R. Baldock, Proc. Cambridge Philos. Soc. 48, 457 (1952).
- ⁸J. Koutecky, Phys. Rev. 108, 13 (1957).
- ⁹L. Künne, Czech. J. Phys. B 17, 894 (1967); Z. Phys. Chem. (Leipzig) 265, 745 (1984).
- ¹⁰B. R. Cooper and A. J. Bennett, Phys. Rev. B 1, 4654 (1970).
- ¹¹S. G. Davison and J. D. Levine, Solid State Phys. 25, 1 (1970).
- ¹²L. Skala, Czech. J. Phys. 27, 171 (1977).
- ¹³M. Steslicka and B. Stankiewicz, Int. J. Quant. Chem. 12, 433 (1977). ¹⁴O. Bilek and P. Kadura, Phys. Status Solidi B 85, 225 (1978).
- ¹⁵(a) For example, M.-H. Whangbo and R. Hoffmann, J. Am. Chem. Soc. 100, 6093 (1978); R. Hoffmann, Rev. Mod. Phys. 60, 601 (1988);
- (b) J. C. Boettger and S. B. Trickey, J. Phys. F 16, 693 (1986); C. Pisani, R. Dovesi, and C. Roetti, in Hartree-Fock Ab Initio Treatment of Crystalline Systems (Springer, Heidelberg, 1988). These particular references are to LCAO methods of the self-consistent type.
- ¹⁶P. Hohenberg and W. Kohn, Phys. Rev. 136, B864 (1964); W. Kohn

- and L. J. Sham, Phys. Rev. 140, A1133 (1965); M. Levy, Proc. Natl. Acad. Sci. U.S.A. 76, 6062 (1979).
- ¹⁷For a recent review, see R. G. Parr and W. Yang, Density-Functional Theory of Atoms and Molecules (Oxford, New York, 1989).
- ¹⁸ N. D. Lang and W. Kohn, Phys. Rev. B 1, 4555 (1970); P. Krüger and J. Pollmann, ibid. 38, 10578 (1988).
- ¹⁹Compare survey in F. Bechstedt and R. Enderlein, Semiconductor Surfaces and Interfaces (Akademie, Berlin, 1988).
- ²⁰ (a) R. A. Marcus, J. Chem. Phys. 98, 5604 (1993); (b) for the continuum normalization for bulk solids, see also J. Callaway, Quantum Theory of the Solid State (Academic, San Diego, 1991).
- ²¹ For example, C. E. D. Chidsey, Science 251, 919 (1991); 252, 631 (1991); C. Miller and M. Gratzel, J. Phys. Chem. 95, 5225 (1991); A. M. Becka and C. J. Miller, ibid. 96, 2657 (1992); R. L. McCarley and A. J. Bard, ibid. 95, 9618 (1991); Y. T. Kim, R. L. McCarley, and A. J. Bard, ibid. 96, 7416 (1992); A. J. Bard, Langmuir 8, 1096 (1992).
- $^{22}\mathrm{Note}$ that this E_s differs slightly from Eq. (2.20) of Ref. 10, due to a different choice of the third vector a₃. In Ref. 10 a₃ is perpendicular to the surface. The direction of a₃ in the present paper is shown in Fig. 1.
- ²³ For example, Ref. 10.
- ²⁴For reviews, see I. L. Spain, Chem. Phys. Carbon 8, 1 (1972); M. Charlier and A. Charlier, ibid. 20, 59 (1987).
- ²⁵J. D. Bernal, Proc. R. Soc. London Ser. A **160**, 749 (1924).
- ²⁶P. R. Wallace, Phys. Rev. **71**, 622 (1947).
- ²⁷C. A. Coulson and R. Taylor, Proc. R. Soc. London Ser. A 65, 815 (1952).
- ²⁸W. M. Lomer, Proc. R. Soc. London Ser. A 277, 330 (1955).
- ²⁹D. F. Johnson, Proc. R. Soc. London Ser. A 277, 349 (1955).
- ³⁰J. C. Slonczewski and P. R. Weiss, Phys. Rev. 109, 272 (1958); J. W. McClure, ibid. 108, 612 (1957).
- ³¹L. G. Johnson and G. Dresselhaus, Phys. Rev. B 7, 2275 (1973).
- ³²G. S. Painter and D. E. Ellis, Phys. Rev. B 1, 4747 (1970).
- ³³ A. Zunger, Phys. Rev. B 17, 626 (1978), where the electronic properties of bulk graphite are calculated using a self-consistent modification of the extended Hückel approximation.
- ³⁴R. C. Tatar and S. Rabii, Phys. Rev. B 25, 4126 (1982).
- ³⁵N. A. W. Holzwarth, S. G. Louie, and S. Rabii, Phys. Rev. B 26, 5382 (1982).
- ³⁶J.-C. Charlier, X. Gonze, and J.-P. Michenaud, Phys. Rev. B 43, 4579 (1991).
- ³⁷Calculations of the isolated AB two-layer of graphite within the localdensity approximation are reported in S. B. Trickey, F. Müller-Plathe, G. H. F. Diercksen, and J. C. Boettger, Phys. Rev. B 45, 4460 (1992). One-layer and two-layer calculations of graphite using the extended Hückel method are given in M. Soto, J. Microsc. 152, 779 (1988); Surf. Sci. 225, 190 (1990).
- ³⁸The coordinates of A_0B_i are given by (1/3, 2/3), (1/3, 1/3), and (-2/3, -1/3), respectively. Consequently, $F_2 = \sum_{i=1}^3 e^{ik_{\parallel} \cdot A_0 B_i} = e^{2\pi i (k_1 + 2k_2)/3} + e^{-2\pi i (2k_1 + k_2)/3} + e^{2\pi i (k_1 - k_2)/3}$.
- ³⁹ For detailed discussion, see Refs. 24 and 30. ⁴⁰ In Eq. (16) terms such as $\Sigma_{l_1 l_2} e^{ik_{\parallel} \cdot (r_l^2 r_p^2)}$ need to be evaluated. By way of illustration, we first calculate this sum for $s=\beta$ and for $i=\alpha$. An α atom, A_0 , possesses three neighboring β atoms in the plane, as in Fig. 5. $\sum_{l_1 l_2} e^{ik_{\parallel} \cdot (r_l^{\beta} - r_{l_1}^{\alpha})} = \sum_{i=1}^{3} e^{ik_{\parallel} \cdot A_0 B_i} = F_2$. Similarly, for $s = \alpha$ and $i = \beta$, $\sum_{l,l,b} e^{i\mathbf{k}_{\parallel}} \cdot (\mathbf{r}_{l}^{\alpha} - \mathbf{r}_{l}^{\beta}) = e^{i\mathbf{k}_{\parallel}} \cdot (\mathbf{B}_{1}\mathbf{A}_{0} + \mathbf{B}_{1}\mathbf{A}_{2} + \mathbf{B}_{1}\mathbf{A}_{3}) = e^{-2\pi i(k_{1} + 2k_{2})/3} + e^{2\pi i(2k_{1} + k_{2})/3}$ $+e^{-2\pi i(k_1-k_2)/3}=F_2^*$, where F_2 is given in Ref. 38.
- ⁴¹B. Källebring, H. Ou-Yang, and R. A. Marcus (unpublished).
- ⁴²R. Hoffmann, J. Chem. Phys. **39**, 1397 (1963).